Predictors of cerebral microembolization during phased radiofrequency ablation of atrial fibrillation: analysis of biophysical parameters from the ablation generator

Short title: Microembolization during phased RF ablations

Edina Nagy-Balo[1]MD, Alexandra Kiss[1]MD, Catherine Condie[2]PhD, Mark Stewart[2]PhD, Istvan Edes[1]MD,PhD, Zoltan Csanadi[1] MD,PhD - (1) University of Debrecen, Institute of Cardiology, Debrecen, Hungary; (2) Medtronic Inc., Minneapolis, Minn, USA

Corresponding author: Edina Nagy-Balo M.D.

Address: Institute of Cardiology, University of Debrecen

22 Móricz Zs. Krt.

Debrecen, Hungary

H-4032

Phone: +36306287720

Fax: +3652414928

E-mail: edinanagybalo@yahoo.com

Conflict of Interest/Disclosures:

The study was partially sponsored by Medtronic Inc., Minneapolis, Minn, USA

Edina Nagy-Baló: none; Alexandra Kiss: none; Cathy Condie: Medtronic Inc. employee; Mark Stewart: Medtronic Inc. employee; István Édes: none; Zoltán Csanádi: speaker honorarium and grant support from Medtronic Inc.

Total word count: 3889

Abstract:

Background: Pulmonary vein isolation with phased radiofrequency current and use of a pulmonary vein ablation catheter (PVAC) has recently been associated with a high incidence of clinically silent brain infarcts on diffusion-weighted MRI, and a high microembolic signal (MES) count detected by transcranial Doppler.

Objective: to investigate the potential correlation between different biophysical parameters of energy delivery (ED) and MES generation during PVAC ablation.

Methods: MES counts during consecutive PVAC ablations were recorded for each ED and time-stamped for correlation with temperature, power and impedance data from the GENius 14.4 generator. Additionally, catheter-tissue contact was characterized by the template deviation score, calculated by comparing the temperature curve with an ideal template representing good contact, and by the respiratory contact failure score, to quantify temperature variations indicative of intermittent contact due to respiration.

Results: A total of 834 EDs during 48 PVAC ablations were analyzed. A significant incease in MES count was associated with a lower average temperature, a temperature integral over 62 $^{\circ}$C, a higher average power, the total energy delivered, higher respiration and template deviation scores ($p<0.0001$), and simultaneous ED to the most proximal and distal poles of the PVAC ($p<0.0001$).

Conclusions: MES generation during ablation is related to different indicators of poor electrode-tissue contact, the total power delivered and the interaction between the most distal and the most proximal electrodes.

KEY WORDS: atrial fibrillation, pulmonary vein isolation, GENius generator, PVAC catheter, cerebral microembolization, transcranial Doppler

LIST OF ABREVIATIONS

PVI – Pulmonary vein isolation

AF – Atrial Fibrillation

SCI – Silent cerebral ichaemia

RF - Radiofrequency

DW – Diffusion weighted

PVAC - Pulmonary vein ablation catheter

TCD – Transcranial Doppler

MES – Microembolic signal

MCA – Middle cerebral artery

CB - Cryoballoon

ED – Energy delivery

LA – Left atrium

ACT – Activated clotting time

Introduction:

Pulmonary vein isolation (PVI) is an established method for the treatment of atrial fibrillation (AF), with a relatively low risk (<1%) of clinical stroke or TIA (1). However, clinically silent cerebral ischemia (SCI) can be detected by diffusion-weighted (DW) MRI in 5-40% of the patients, depending on the ablation technology used (2-7). The highest incidence of SCI during PVI has been reported on the use of phased radiofrequency (RF) and the circular multipolar pulmonary vein ablation catheter (PVAC) (6,7). While DW MRI is the gold standard for the demonstration of cerebral lesions postablation, transcranial Doppler (TCD) can be used to detect microembolic signals (MESs) in the middle cerebral arteries (MCAs) during the procedure. In line with the MRI results, we earlier detected a significantly higher number of MESs during PVAC ablations than with the use of a cryoballoon (CB). Importantly, the majority of the MESs were demonstrated to be generated during the energy delivery (ED) phase of PVAC ablations (8).

Limited data are available regarding the mechanism of MES generation during RF ablation. In this study, we compared the MES counts recorded during ED with the high-resolution biophysical data collected from the generator during phased RF ablation in a consecutive series of patients. We hypothetized, that some biophysical data specific to this multielectrode ablation technology were potentially related to microembolization. These included the number of electrodes on and the unipolar/bipolar ratio during ED, the simultaneous use of the most proximal and the most distal electrodes during RF applications and metrics indicating poor or variable electrode-tissue contact.

Methods

Study population, patient preparation:

Forty-eight consecutive patients undergoing PVI for symptomatic paroxysmal or persistent AF not adequately controlled by at least one antiarrhythmic drug were eligible for inclusion in the study. Exclusion criteria included long-standing persistent AF, known bleeding disorders and a contraindication to oral anticoagulation. The study conformed with the guiding principles of the Declaration of Helsinki, and were approved by the Institutional Ethics Committee. All patients provided their signed written informed consent prior to inclusion.

On the day before ablation transesophageal echocardiography was performed to exclude the presence of a cardiac thrombus. All patients received oral anticoagulation before the PVI, with a target international normalized ratio of 2.0 to 3.0, which was maintained for the procedure.

Ablation protocol:

All procedures were performed under conscious sedation, using midazolam and fentanyl. The ablation protocol was performed as reported earlier (8). Briefly, decapolar and quadripolar catheters were advanced from the femoral vein and positioned in the coronary sinus and the right ventricle. A single transseptal puncture was performed under fluoroscopic and intracardiac echocardiographic guidance, using a standard technique. A deflectable 12 Fr long sheath (FlexCath, Medtronic CryoCath LP, Kirkland, Quebec, Canada) was used in the left atrium (LA) and flushed continuously with heparinized saline. This sheath was used to guide the PVAC (Ablation Frontiers, Medtronic, Carlsbad, CA, USA) catheter. Immediately before transseptal puncture, a 150 IU/kg body weight iv heparin bolus was given, followed by a continuous infusion to maintain a minimum activated clotting time (ACT) target level of

350 s. ACT was always checked prior to the first ablation and every 20 min thereafter. Additional 2000-5000 IU iv boluses of heparin were administered as required to reach the minimum target ACT level.

The PVAC was connected to a duty-cycled RF generator (GENius™ 14.4, Ablation Frontiers, Medtronic, Carlsbad, CA, USA). The system is capable of ED in a temperature-controlled mode with simultaneous application on all or any selected number of the 10 electrodes. All ablations were performed at a 60 degree temperature goal for 1 minute., and a maximum power at 10 W. It is noteworthy that there is a possibility of a significant interaction of the current densities in electrode 1 (E1) and electrode 10 (E10) when these are in close proximity (9) evidenced by an impedance drop below 110 Ohms (10). Simultaneous ED on these poles was therefore attempted only after fluoroscopic assessment of the interelectrode distance, which was considered adequate if the space between E1 and E10 was at least double the usual 3-mm interelectrode distance as assessed from multiple views. Examples of a satisfactory catheter position and one where E1 and E10 were too close are shown in Figure 1. RF energy was applied for 60 s, usually 3-4 times per PV starting with a bipolar/unipolar ratio of 4:1. Any electrode pair that failed to reach at least 50 ^{o}C during RF delivery was switched off to avoid ineffective ED due to improper contact at the electrode-tissue interface. Furthermore, when any electrode reached the target temperature while delivering very low power (1-2 W), it was considered a sign of an undesirably strong electrode-tissue contact or a wedge position of the electrode, and ED to that particular electrode was switched off.

The endpoint was electrical isolation of all PVs, confirmed by demonstrating an entrance block.

TCD recording and evaluation:

TCD recording was performed throughout the period of LA access. The transducer was held in place by a proprietary headpiece supplied with the system. The MCAs were insonated bilaterally from transtemporal windows by using a multifrequency Doppler (Multi Dop T digital, DWL, QL software 2.8). The TCD parameter settings recommended by the consensus criteria (11) were maintained constant during the procedures. The insonation depth was 45-55 mm, the sample volume was 8 mm, and the power was 60-100 mW. MES counts were recorded for each ED and time-stamped to correlate with the high resolution power and temperature parameters collected from the GENius 14.4 generator for off-line analysis.

Data collection from the GENius 14.4 generator:

Generator files for each ablation during the procedure were collected. The files included information on the ablation (mode, electrodes enabled), the power for each electrode sampled at 1 Hz, and the temperature for each electrode sampled at 8 Hz. Parameters analyzed off-line for potential correlation with the MES data included the bipolar/unipolar ratio, the average power delivered, the total energy delivered, the number of electrodes on during the ED, the simultaneous use of E1 and E10, the average temperature, and the presence of a temperature overshoot. A temperature overshoot was defined as $\geq 62\ ^{\circ}C$ during the ED, and the integral over $62\ ^{\circ}C$ was calculated as the area under the temperature curve above $62\ ^{\circ}C$.

For the evaluation of the electrode-tissue contact, two additional metrics were calculated. The respiratory contact failure score was based on the analysis of temperature variability at respiration frequency in order to quantifiy improper contact attributed to respiratory movements (Figure 2). This score was calculated for each electrode, by filtering

the temperature signal and then calculating the power spectrum at the respiration frequency between 10 and 20 breaths per minute. The other parameter was the template deviation score, which compared the actual temperature curve during ablation with an ideal template. The ideal template was created from in vitro results featuring a quick temperature rise with the target temperature of 60 °C reached within 20 seconds, followed by a steady state for the remainder of the ablation. Template deviation was considered negative in the case of a slow rise or if the temperature remained <60 °C, and positive for a quick temperature rise, and a temperature >60 °C. This concept is outlined in the online supplement on Figure 1, with real examples of an ideal temperature curve and a negative deviation on Figure 2. Template deviation scores were calculated as the sum of the squared errors between the real electrode temperature and the ideal template at each time point for each electrode during ED. The score for each RF delivery representing the mean of the electrodes was related to the MES count.

Statistical analysis:

Gaseous and solid signal counts were summed (total MES). As bilateral recording of MCA was not possible in all cases, mean MES counts per MCA were calculated, using either the mean of the bilateral counts when both sides were measured, or the unilateral data when only one side was available To improve normality, signal count data were natural log-transformed, and ablation parameters were transformed by using whichever formula (square, square root or natural log) provided the closest fit to a normal distribution.

Relationships between ablation parameters and total MES count were descriptively quantified using unadjusted Pearson's correlation coefficients (r) as a first approach.

For in-depth analysis multilevel mixed-effects linear regression was used to evaluate the effect of ablation parameters on the total MES count. Models were adjusted for total energy delivered and average temperature. Interaction terms were used to assess effect

heterogeneity across levels of potential effect-modifying factors. Fixed effects were expressed as estimated differences in the log-transformed outcome, 95% confidence intervals, and p values. Model checking was based on inspection of the normality of residuals.

Applications were excluded from the analysis if temporary signal problems on the TCD occurred. Additionally, energy delivery sessions interrupted earlier than 40 seconds were excluded from the respiratory contact failure, the template deviation and the number of active electrodes analyses.

p values less than 0.05 were interpreted as indicating statistical significance. The statistical package Stata (StataCorp 2009.Stata Statistical Software: Release 11., College Station, TX: StataCorp LP) was used for statistical analysis.

Results:

A total of 834 RF application sessions were performed during phased RF ablation with the PVAC in 48 patients. All patients had an INR value above 2.0 confirmed on the day of the procedure. 6 patients had values slightly above 3.0 but below 4. Bilateral TCD recording could not be achieved in 5 patients. The right side was missing on 4 of these patients, whereas the left side was missing in 1 patient. The mean MES count per ablation did not differ significantly in the unliateral group as compared to patients with bilateral TCD monitoring. (22 SD:32 vs. 28 SD:48 mean MES per ablation, respectively, $p>0.05$).

The number of concomitantly active electrodes during ED was found to increase the MES count significantly (Pearson Correlation Coefficient $r=0.252$, adjusted $p<0.0001$; Figure 3). Accordingly, increase of the total energy delivered to all active poles correlated with an

increase in MES count (Pearson Correlation Coefficient r=0.340, adjusted p<0.0001; Figure 4).

RF energy was delivered simultaneously on E1 and E10 in 285 instances with an impedance drop below 110 Ohm observed in 3 cases. Concomitant use of E1 and E10 resulted in significantly higher MES counts than in ablations where these two poles were not coactive (mean MES per patient 36.3 SD:51.4 vs. mean MES 23.8 SD:38.3 Pearson Correlation Coefficient r=0.160, adjusted p<0.0001).

Both lower average temperatures (in the range 45-55 ˚C) and a higher temperature integral over 62 ˚C resulted in an increased MES count (Figure 5, Pearson Correlation Coefficient r=0.257, 0.145, respectively, adjusted p<0.0001). Moreover, higher temperature integrals over 62 ˚C were found in those ablations where the average temperature was in the range 45-55 ˚C.

Positive template deviation scores did not affect the MES count (Pearson Correlation Coefficient r=0.110, adjusted p=0.342). Negative template deviation scores were associated with an increase in MES count (Figure 6; Pearson Correlation Coefficient r=0.323, adjusted p<0.0001). Higher respiratory contact failure was associated with higher MES count. (Figure 7, left; Pearson Correlation Coefficient r=0.165, adjusted p=0.0002), while an inverse relationship was found between the respiratory contact failure score and the average temperature (Figure 7, right; Pearson Correlation Coefficient r=0.389, adjusted p<0.0001).

No significant relationship was found between the MES count and the bipolar/unipolar ablation mode: mean MES per patient: 26.7 SD:43.6, 28.2 SD:44.3 and 25.2 SD:28.37 were found during EDs with 4:1, 2:1 and 1:1 bipolar:unipolar modes, respectively (Pearson Correlation Coefficient r=0.051, adjusted p=0.35).

Discussion:

Recent reports of SCI during catheter ablation for AF raised concern regarding the safety of these procedures. Although several clinical and procedural predictors of both manifest and silent cerebral embolization have been identified, the direct correlation between thrombus formation and the biophysical parameters during RF ED in the LA is poorly understood. Our data, collected at a high sampling rate from the GENius 14.4 generator with simultaneous recording of MESs during PVI, provide information on multiple aspects of cerebral microembolization.

As previous MR data indicated that the phased RF technology with the PVAC might be more thrombogenic as compared with irrigated RF ablation, our analysis was focused on some distinctive features of this technology.

The E1-E10 interaction is the only known predictor of new lesions on DW MRI after a phased-RF ablation (10,11). Furthermore we recently demonstrated that the number of microemboli detected by TCD during PVI was higher on the concomitant use of E1-E10 (8). This is probably due to a reduced interelectrode distance or electrode overlap when the PVAC loop is compressed which may result in an increased local current density and thereby increased MES production. Significantly higher MES counts with coactive E1 and E10 were also demonstrated in this study, despite a careful fluoroscopic assessement of the electrode positions. We propose two possible explanations: (a) the E1-E10 interaction was due to catheter displacement resulting in a shortened E1-E10 distance during the ablation; (b) the E1-E10 combination was used almost exclusively when most of the electrodes were also enabled, resulting in a higher total energy delivery which was an independent predictor of MES production in this study. Importantly, an impedence drop below 110 Ohms, considered

an indication for E1-E10 interaction by Wieczorek et al (10) occured in a negligible number of energy deliveries in our study.

A specific feature of duty-cycled ablation with the PVAC is RF delivery with different bipolar/unipolar mode ratios. The study by Haines et al. (12) revealed significantly lower MES count and microembolic volume with the unipolar mode than with any of the ED modes with a bipolar component. The unipolar mode was not used in this study and, in accord with our previous results (8), no significant difference in the MES count was found during ED in 4:1 vs. 2:1 mode.

Intermittent contact has also been proposed as a potential mechanism of embolus formation during ED. This appears to be the first investigation of the role of improper tissue-catheter contact in microembolus production during RF ablation. It is known that lower average temperatures achieved with a non-irrigated catheter usually indicate an improper electrode-tissue contact, and higher power is necessary to achieve the target temperature in these instances. Moreover, in the event of intermittent contact, the power increase during the off-contact period can lead to a temperature overshoot once better tissue contact is established (13). We therefore evaluated the average power, average temperature and temperature integral over 62 $^{\circ}$C as indicators of the electrode-tissue contact. To further characterize the contact during ED, a template deviation score was used to quantify the difference between an ideal and the real temperature. As contact problems may relate to respiration, a respiratory contact failure score was also calculated to analyze the temperature variability at the respiration frequency. All of these metrics demonstrated a significant correlation with embolus formation: a lower average temperature (45-55 $^{\circ}$C), a higher average power, a higher temperature integral over 62 $^{\circ}$C, a higher template deviation score and a higher respiratory contact failure score were independent predictors of an increased MES count. Of note, all

ablation procedures were performed under conscious sedation in this study. Ventillation under general anesthesia might result in different respiratory variability and MES count.

Contact becomes especially critical when multipolar ablation catheters are used. It is important, that the simultaneous attainment of sufficient electrode-tissue contact on multiple poles, with either a circular or a linear arrangement, may not be feasible in the majority of cases due to the complex anatomy. Modifications in the power handling of the RF generator to ensure a gradual and limited increase during temporary no contact scenarios, which has been implemented in the most recent software version of the GENius generator may prove to be useful to avoid high-temperature peaks when better contact is reestablished. Another, although technically ponderous strategy which could be beneficial is the incorporation of contact force sensors in these electrodes thereby enabling the assessment of contact before an electrode is selected for RF delivery. Moreover, the overall delivered energy is necessarily higher with simultaneous ablation on multiple electrodes, and our data reveal that the higher the total energy delivered, the greater the number of emboli. It could be argued, however, that, with the longer lesion created by applying RF to multiple poles, fewer ED sessions are required. However, it is unknown whether the total MES count itself is related to the thrombogenic potential of the ablation procedure, or whether the intensity of MES formation (the MES count in a given time) is also of importance.

Another problem specific to the circular catheter design is the potential interaction between the electrodes if the circle is compressed and the poles mounted on the proximal and distal parts of the circle come closer to each other. A possible solution to prevent this interaction, software regulation of the ablator, has already been implemented in the latest version of the GENius generator (software version 15.0), which does not allow simultaneous ED on E1-E10. However. an interaction between other poles in case of a wedged position

remains still possible, therefore careful assessment of the electrode position is still not obsolete.

Limitations:

Our study has significant limitations. This was a retrospective analysis with the off-line correlation of data recorded by the RF generator and TCD. The data reflect only one technology, with limited implications for other techniques, although contact metrics and their relationship with embolization are likely to apply for RF ablation in the LA, regardless of the technology.

Conclusions:

Cerebral microembolization during ED with the PVAC catheter was associated with the total energy delivered and several biophysical parameters which can be linked to a variable or poor electrode-tissue contact: lower average temperature, negative template deviation score, temperature overshoots, respiratory contact failure score and increased average power. Concomitant RF delivery to electrodes potentially moving in close proximity to each other also accounts for MES formation.

Acknowledgement:

We are grateful to Dr. David E Haines M.D. for his advice and help in the preparation of this manuscript.

Reference:

1. Kok LC, Mangrum JM, Haines DE, Mounsey JP. Cerebrovascular complication associated with pulmonary vein ablation. J CardiovascElectrophysiol. 2002;13:764-767.
2. Schrickel JW, Lickfett L, Lewalter T, Mittman-Braun E, Selbach S, Strach K, Nahle CP, Schwab JO, Linhart M, Andrie R, Nickenig G, Sommer T. Incidence and predictors of silent cerebral embolism during pulmonary vein catheter ablation for atrial fibrillation. Europace. 2010;12:52-57.
3. Gaita F, Caponi D, Pianelli M, Scaglione M, Toso E, Cesarani F, Boffano C, Gandini G, Valentini MC, De Ponti R, Halimi F, Leclercq JF. Radiofrequency catheter ablation of atrial fibrillation: A cause of silent thromboembolism? Magnetic resonance imaging assessment of cerebral thromboembolism in patients undergoing ablation of atrial fibrillation. Circulation. 2010;122:1667-1673.
4. Neumann T, Kuniss M, Conradi G, Janin S, Berkowitsch A, Wojcik M, Rixe J, Erkapic D, Zaltsberg S, Rolf A, Bachmann G, Dill T, Hamm CW, Pitschner HF. Medafi-trial (micro-embolization during ablation of atrial fibrillation): Comparison of pulmonary vein isolation using cryoballoon technique vs. radiofrequency energy. Europace. 2011;13:37-44.
5. Lickfett L, Hackenbroch M, Lewalter T, Selbach S, Schwab JO, Yang A, Balta O, Schrickel J, Bitzen A, Luderitz B, Sommer T. Cerebral diffusion-weighted magnetic resonance imaging: A tool to monitor the thrombogenicity of left atrial catheter ablation. J Cardiovasc Electrophysiol. 2006;17:1-7.
6. Siklódy C. H., T. Deneke, M. Hocini, H. Lehrmann, D.I. Shin, S. Miyazaki, S. Henschke, D. Kalusche, M. Haissagure, T. Arentz. Incidence of asymptomatic

embolic events following pulmonary vein isolation procedures: comparison between different ablation devices. J Am Coll Cardiol. 2011;58:681-688.

7. Gaita F, Leclercq JF, Schumacher B, Scaglione M, Toso E, Halimi F, Schade A, Froehner S, Ziegler V, Sergi D, Cesarani F, Blandino A. Incidence of silent cerebral thromboembolic lesions after atrial fibrillation ablation may change according to technology used: Comparison of irrigated radiofrequency, multipolar nonirrigated catheter and cryoballoon. J Cardiovascular Electrophysiol. 2011;22:961-968.
8. Nagy-Baló E, Tint D, Clemens M, Beke I, Kovács RK, Csiba L, Édes I, Csanádi Z. Transcranial Measurement Of Cerebral Microembolic Signals During Pulmonary Vein Isolation: A Comparison Of Two Ablation Techniques.Circ Arrhythm Electrophysiol.2013;6:473-480
9. Wieczorek M, Lukat M, Hoeltgen R, Condie C, Hilje T, Missler U, Hirsch J, Scharf C. Investigation into Causes of Abnormal Cerebral MRI Findings Following PVAC Duty Cycled Phased RF Ablation of Atrial Fibrillation. J. Cardiovasc. Electrophysiol. 2013; 24 (2): 121-128.
10. Haines DE, Stewart MT, Ahlberg S, Condie C, Fiedler GR, Halimi F, Deneke T. Etiology of microemboli production during ablation with irrigated RF and multipolar phased RF ablation. Heart Rhythm 2012; 9(5), S73.1-5.
11. Ringelstein EB, Droste DW, Babikian VL, Evans DH, Grosset DG, Kaps M, Markus HS, Russell D, Siebler M.Consensus on microembolusdetection by TCD. International Consensus Group on MicroembolusDetection. Stroke.1998;29:725-729.
12. Haines DE, Stewart MT, Ahlberg S, Barka ND, Condie C, Fiedler GR, Kirchhof NA, Halimi F, Deneke T. Microembolism and catheter ablation I: a comparison of irrigated radiofrequency and multielectrode-phased radiofrequency catheter ablation of pulmonary vein ostia. Circ. Arrhythm. Electrophisiol.2013;6:16-22.

13. Wittkampf FH, Nakagawa H. RF catheter ablation: Lessons on lesions. Pacing Clin Electrophysiol. 2006; 29:1285-1297.

Figure Legend

Figure 1. Position of the PVAC catheter during ED

Panel A indicates the optimal catheter position ensuring at least a doubleE1-E10 interelectrode distance compared with the distance between the nonmodifiable poles. Panel B shows a catheter position where E1 and E10 are unsafely close.

Figure 2. Respiration-related temperature variability

Temperature signal oscillation can be seen in the temperature curves of electrodes 6, 9 and 10 as a marker of an intermittent contact at respiratory frequency (red lines). The absolute values of the respiratory contact failure score are also indicated for each of the 10 electrodes demonstrating the highest scores for electrodes 6,9,10.

Figure 3. MES count and the number of active electrodes

Figure 4. Association of the total energy delivered on all active electrodes with the MES count

Figure 5. Effects of average temperature (left) and temperature integral over 62 ˚C (right) on the MES count.

Figure 6. Association of template deviation score with MES count

Figure 7. Effects of respiration score on MES count (left) and temperature (right)

See text for details.

FIGURES

Figure 1.

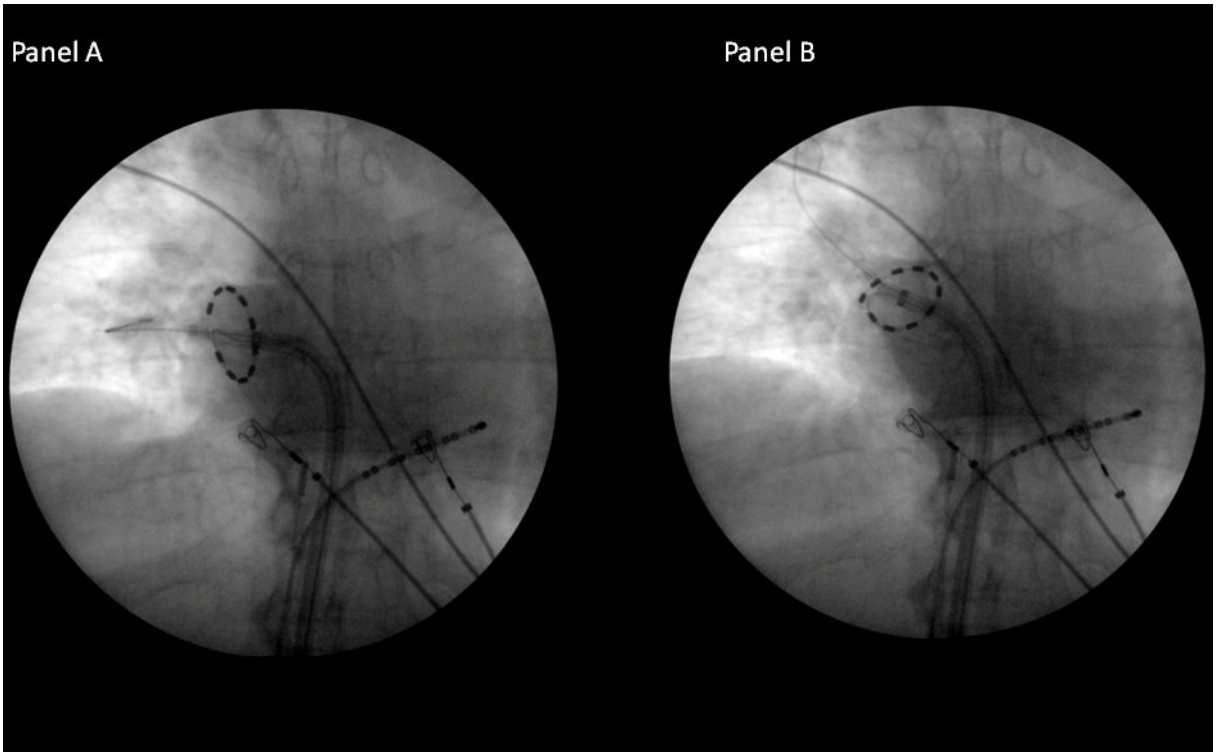

Figure 2.

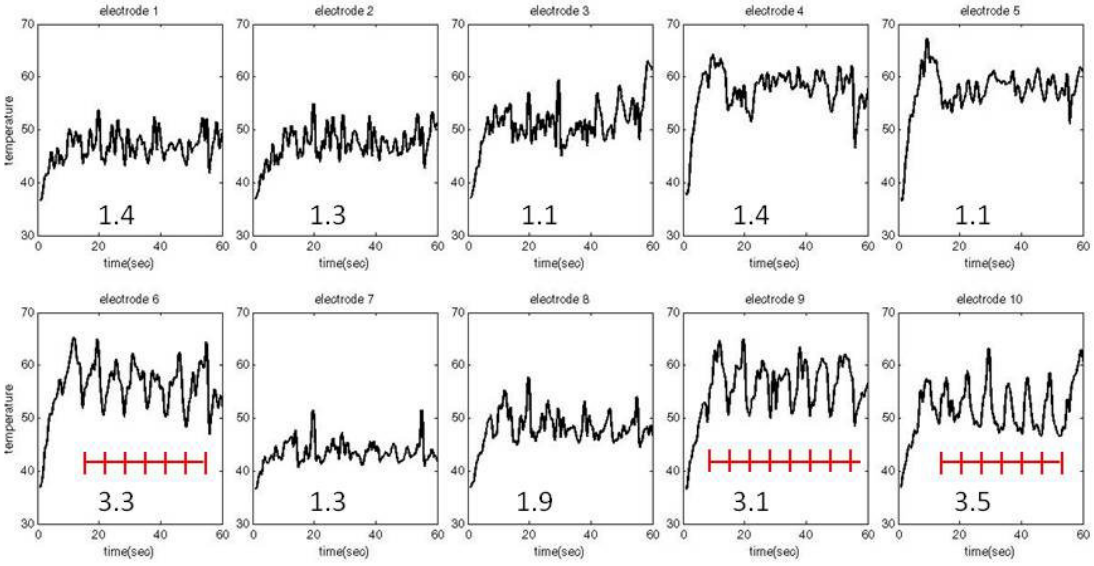
electrode 1
electrode 2
electrode 3
electrode 4
electrode 5
electrode 6
electrode 7
electrode 8
electrode 9
electrode 10
temperature
time(sec)
1.4
1.3
1.1
1.4
1.1
3.3
1.3
1.9
3.1
3.5

Figure 3.

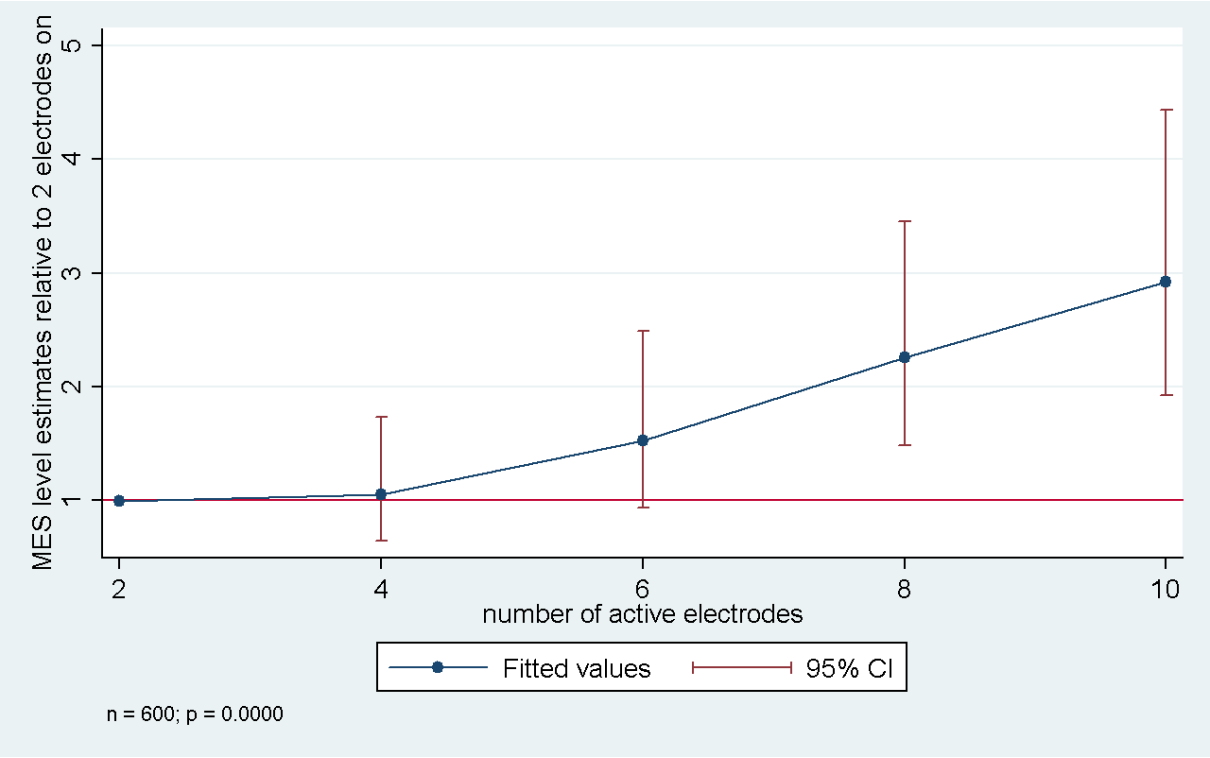
MES level estimates relative to 2 electrodes on
1
2
3
4
5
2
4
6
8
10
number of active electrodes
Fitted values
95% CI
n = 600; p = 0.0000

Figure 4.

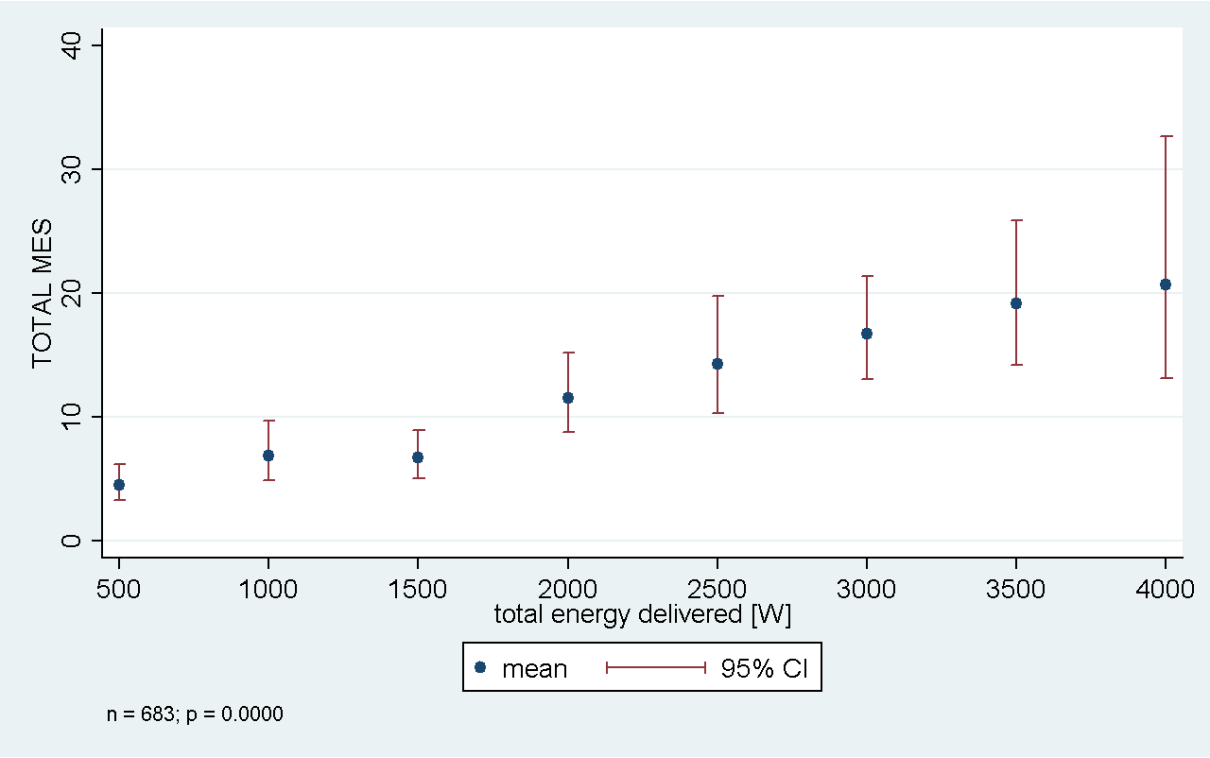
TOTAL MES
0
10
20
30
40
500
1000
1500
2000
2500
3000
3500
4000
total energy delivered [W]
mean
95% CI
n = 683; p = 0.0000

Figure 5.

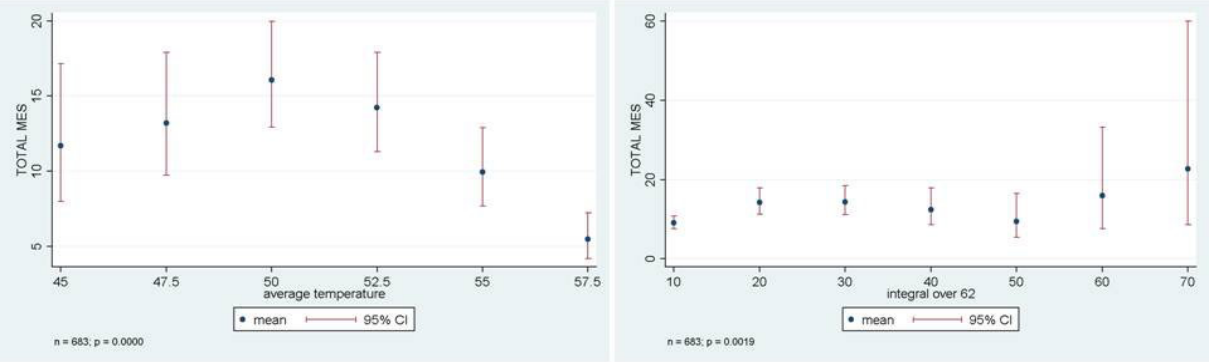
TOTAL MES
5
10
15
20
45
47.5
50
52.5
55
57.5
average temperature
mean
95% CI
n = 683; p = 0.0000
TOTAL MES
0
20
40
60
10
20
30
40
50
60
70
integral over 62
mean
95% CI
n = 683; p = 0.0019

Figure 6.

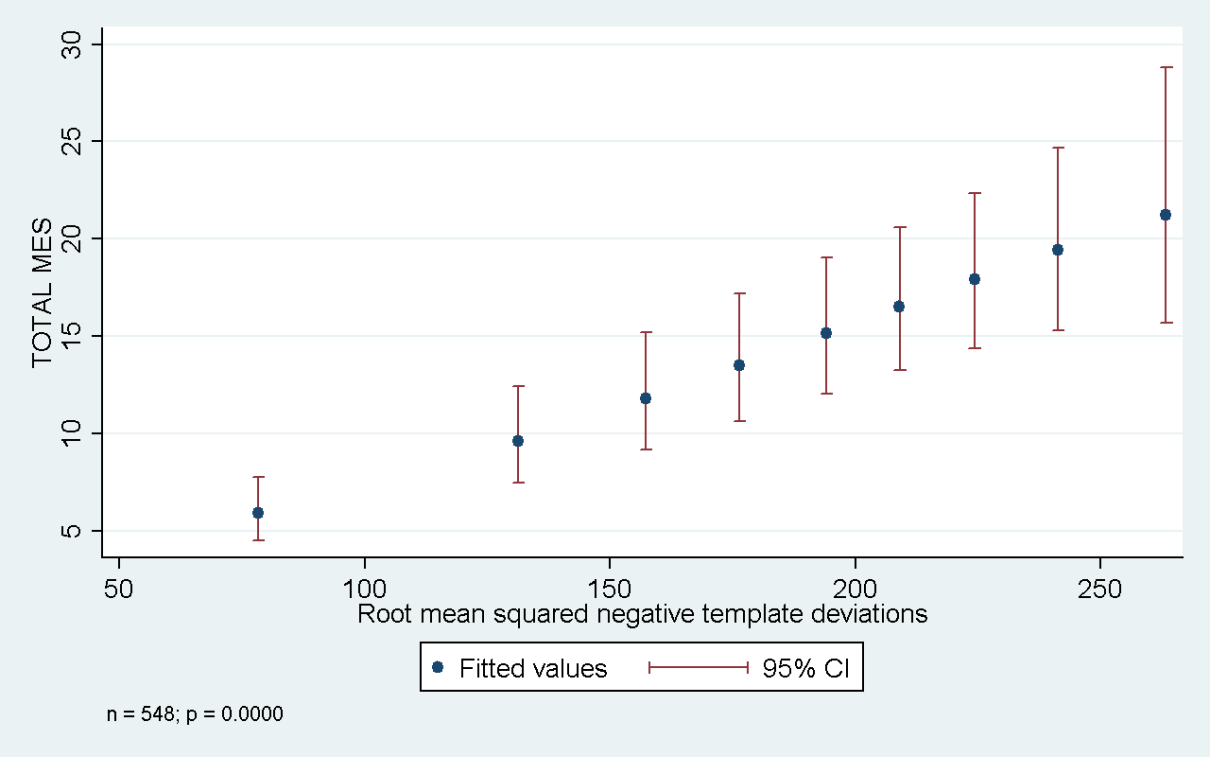
TOTAL MES
5
10
15
20
25
30
50
100
150
200
250
Root mean squared negative template deviations
Fitted values
95% CI
n = 548; p = 0.0000

Figure 7.

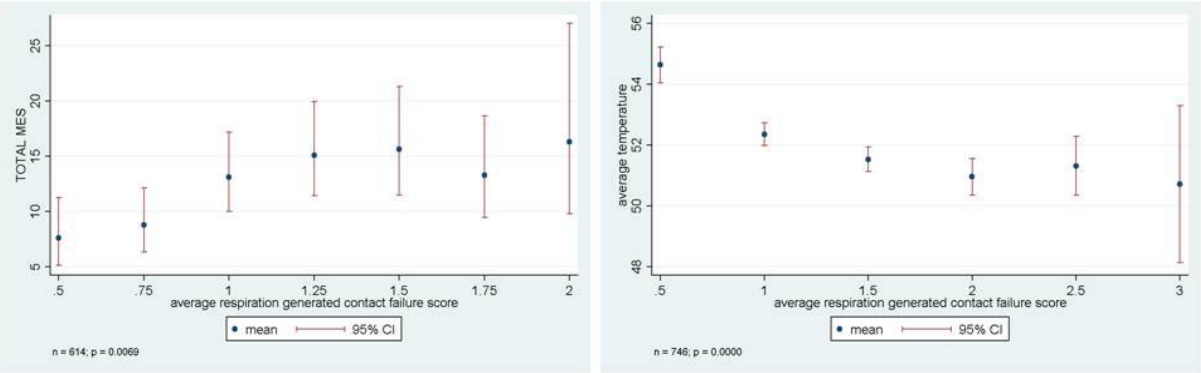
TOTAL MES
5
10
15
20
25
.5
.75
1
1.25
1.5
1.75
2
average respiration generated contact failure score
mean
95% CI
n = 614; p = 0.0069
average temperature
48
50
52
54
56
.5
1
1.5
2
2.5
3
average respiration generated contact failure score
mean
95% CI
n = 746; p = 0.0000

Figure Legend

Figure 1. Position of the PVAC catheter during ED

Panel A indicates the optimal catheter position ensuring at least a doubleE1-E10 interelectrode distance compared with the distance between the nonmodifiable poles. Panel B shows a catheter position where E1 and E10 are unsafely close.

Figure 2. Respiration-related temperature variability

Temperature signal oscillation can be seen in the temperature curves of electrodes 6, 9 and 10 as a marker of an intermittent contact at respiratory frequency (red lines). The absolute values of the respiratory contact failure score are also indicated for each of the 10 electrodes demonstrating the highest scores for electrodes 6,9,10.

Figure 3. MES count and the number of active electrodes

Figure 4. Association of the total energy delivered on all active electrodes with the MES count

Figure 5. Effects of average temperature (left) and temperature integral over 62 °C (right) on the MES count.

Figure 6. Association of template deviation score with MES count

Figure 7. Effects of respiration score on MES count (left) and temperature (right)

See text for

SUPPLEMENTAL MATERIAL

Figure 1.

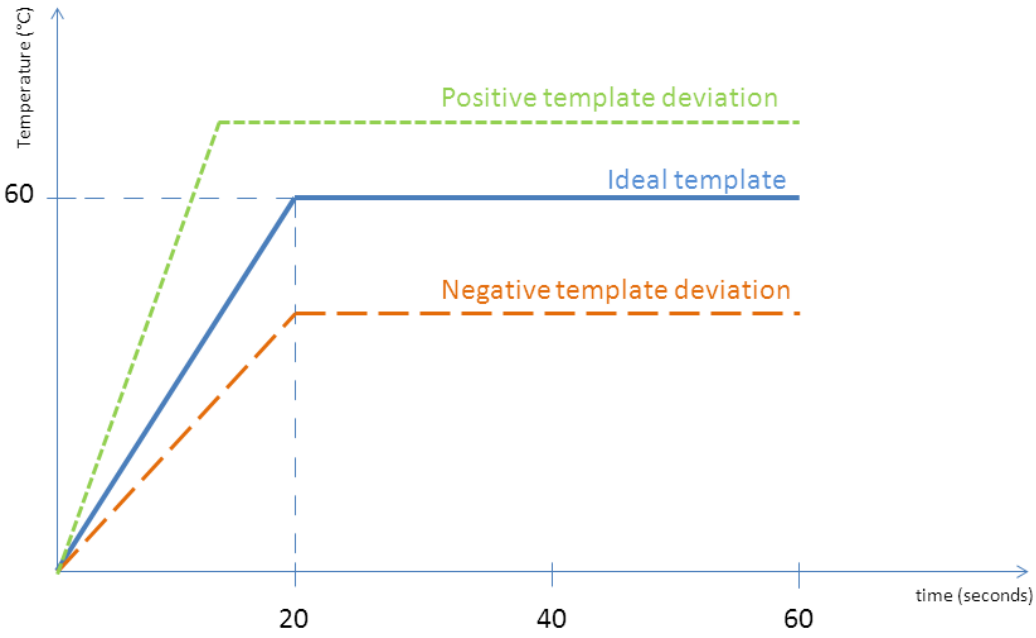

Figure 2.

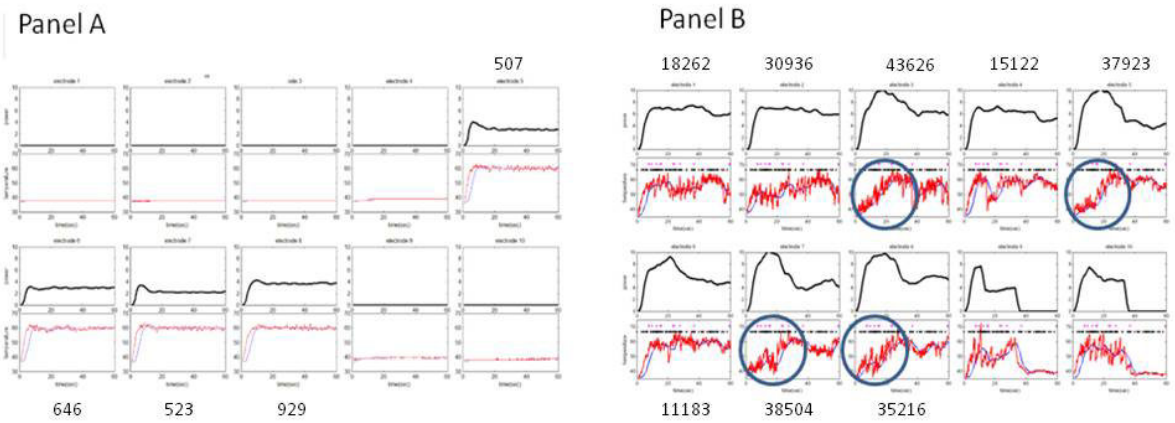
Panel A
507
646
523
929
Panel B
18262
30936
43626
15122
37923
11183
38504
35216

SUPPLEMENTAL MATERIAL LEGEND

Figure 1. Schematic illustration of the ideal temperature template and temperature curves with positive and negative deviations during ED

See text for details

Figure 2. Temperature curves during energy delivery

Panel A shows ideal temperature curves on electrodes 5-8, where the target temperature of 60 °C is achieved quickly and it remains constant for the rest of the energy delivery period. Panel B demonstrates examples for negative template deviations with a slow rise of the temperature at the beginning of ablation on electrodes 3,5,7,8 (circle) and temperature values below the ideal. The absolute values of template deviation scores are given for all electrodes which were active during the entire energy delivery session.